Liquid crystal polyimides: 17. Thermotropic poly(ester imide)s based on trimellitimide and diamino oligoether spacers

Javier de Abajo and José G. de la Campa
Instituto de Polimeros, CSIC, Juan de la Cierva 3, E-28006 Madrid, Spain

and Hans R. Kricheldorf* and G. Schwarz
Institut für Technische und Makromolekulare Chemie, Universität Hamburg, Bundesstr. 45, D-20146 Hamburg, Germany

(Received 11 April 1994; revised 18 July 1994)

Two symmetrical imide diacids were prepared from trimellitic anhydride and two α,ω-diamines containing ether linkages, namely 1,8-diamino-3,6-dioxaoctane and 1,12-diamino-4,9-dioxadodecane. Polycondensations in the melt of the imide diacids and diacetyl bisphenols yielded the corresponding series of poly(ester imide)s (PEIs), characterized by an alternating sequence of stiff, aromatic imide units and ether-containing aliphatic spacers. The presence of –O– linkages within the flexible spacers greatly affected the thermal transitions and the thermotropic behaviour of the PEIs. Comparison with homologous PEIs without ether linkages revealed lower glass transition temperatures and a weaker tendency to form liquid crystal mesophases. Only the PEIs from 4,4′-dihydroxybiphenyl showed a regular thermotropic behaviour, as could be proved by optical microscopy with crossed polarizers, by d.s.c. and by synchrotron radiation measurements at variable temperature. These PEIs form layer structures in the solid and liquid state. The textures suggest the formation of a smectic-A phase.

(Keywords: poly(ester imide)s; synthesis; thermotropic behaviour)

INTRODUCTION

The systematic study of thermotropic poly(ester imide)s (PEIs) has allowed reliable structure–liquid crystal (LC) behaviour relationships to be established for this class of polymeric materials in recent years. Thus, in previous work it was found that symmetrical bis-trimellitimide monomers containing aliphatic spacers (**1**) produce LC polyimides when polycondensed with rigid bisphenols[1,2]. Furthermore, thermotropic polyesters have been reported containing oligo ethylene glycol sequences as spacers and aromatic dicarboxylic acids free of imide groups as mesogens[3–7]. The presence of ether linkages within the spacer chain did not disturb the formation of a smectic phase and only the phase transition temperatures were affected on substituting oligo ethylene glycol spacers by polymethylene spacers.

In contrast, recent results of this series have proved that the presence of ether linkages within the spacer chain does drastically reduce the ability of PEIs derived from *N*-(4′-carboxyphenyl) trimellitimide to form layered supramolecular structures[8]. Therefore, it is interesting to know whether ether-containing spacers also prevent the formation of smectic LC polyimides when symmetrical bis-trimellitimides are used.

In order to perform a consistent study of the structural factors governing the thermotropic behaviour of these polymers, PEIs prepared from monomers **2** and **3** and various bisphenols will be compared with those of the family prepared from **1**, $n=8$ or 12, and bisphenols previously reported[1,2]. Thus, the aims of this work consisted mainly of the elucidation of the differences between homologous polymers from monomers **2** or **3** and monomer **1**, $n=8$ or 12, taking into consideration structural characteristics to explain the formation and stabilization of mesomorphic, layered supramolecular structures.

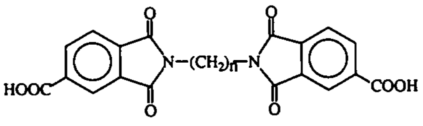

1 (n = 4 - 12)

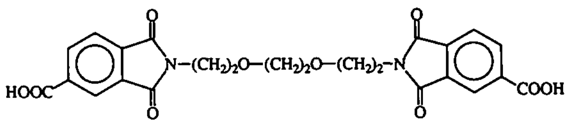

2

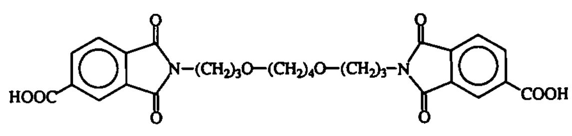

3

---

* To whom correspondence should be addressed

0032-3861/94/25/5577–09

EXPERIMENTAL

Materials

Trimellitic anhydride was donated by Glasurit SA (Guadalajara, Spain) and was used without purification. 1,8-Diamino-3,6-dioxaoctane (DDO) and 1,12-diamino-4,9-dioxadodecane (DDD) were purchased from Aldrich, and used as received. Diacetyl bisphenols were prepared from the corresponding bisphenols by treatment with acetic anhydride, by the general method described by Richard[9]. They were then recrystallized from suitable solvents.

Synthesis of imide monomers 2 and 3

The symmetrical diacid imides from DDO and DDD were prepared by the following synthetic route: trimellitic anhydride (0.2 mol) was dissolved in acetic acid (600 ml) at 50–60°C to obtain a clear solution of the anhydride. Upon cooling at room temperature in a water bath, diamine (0.1 mol) was slowly added in such a way that the temperature of the mixture did not rise over 25°C. After stirring at this temperature for 1 h, the mixture was stage heated up to 120°C and maintained at this temperature for 4 h. The solution was precipitated into water/ice to give the crude diacid imide as a white powder, which was subsequently thoroughly washed with cold water and dried. Yields of several operations ranged between 55% and 65%. After recrystallization from dioxane/hexane (2/1, v/v) the diacid imide from DDO (**2**) showed a melting point of 209–210°C, and that from DDD (**3**) showed a melting point of 156–157°C, after recrystallization from H_2O/ethanol, (1/1, v/v).

Analyses for **2**, $C_{24}H_{20}N_2O_{10}$ (496.43): calculated: C 58.06, H 4.03, N 5.65. Found: C 57.98, H 4.25, N 5.48.

^1H n.m.r. (δ, ppm, measured in DMSO-d_6): 8.30, 2H (d), 7.93, 2H (s), 7.93, 2H (d), 3.67, 4H (t), 3.53, 4H (t), 3.45, 4H (s).

Analyses of **3**, $C_{28}H_{28}N_2O_{10}$ (552.54): calculated: C 60.87, H 5.07, N 5.07. Found: C 60.58, H 5.20, N 5.27.

^1H n.m.r. (δ, ppm, measured in DMSO-d_6): 8.31, 2H (d), 8.20, 2H (s), 7.81, 2H (d), 3.85, 4H (t), 3.48, 4H (t), 3.36, 4H (t), 1.98, 4H (m), 1.49, 4H (t).

Polycondensations

All polycondensations were conducted in a cylindrical, round-bottom, glass vessel equipped with gas inlet and outlet tubes and mechanical stirrer. The general method was as follows: diacid imide (~30 mmol) and an equimolar amount of a diacetylated bisphenol and magnesium oxide (30 mg), were progressively heated under a blanket of nitrogen up to 220–230°C, when the reaction started and evolution of acetic acid began. The molten mixture was stirred for 2 h at that temperature, and then at 250–260°C for 1 h, whereby most acetic acid was removed. Finally, the mixture was heated to 280°C under vacuum for 30–60 min. In order to avoid thermal degradation, the temperature was never raised above 280°C, albeit several PEIs solidified in the course of the reaction. After cooling, the polymers were dissolved in a mixture of methylene chloride (CH_2Cl_2) and trifluoroacetic acid (TFA) (4:1), the solution was filtered through Celite® and finally precipitated with cold methanol. After isolation by filtration, the polymers were thoroughly washed with methanol and dried in vacuum at 80°C.

Measurements

Inherent viscosities were measured with an automated Ubbelohde viscometer thermostatically controlled at 25°C, on 0.5% (w/v) polymer solutions in CH_2Cl_2:TFA (4:1).

D.s.c. measurements were carried out using a Perkin–Elmer DSC-4 with samples in aluminium pans under nitrogen at a heating rate of 20°C min^{-1}.

The wide-angle X-ray scattering (WAXS) curves were measured with a powder diffractometer (Siemens D-500), using Ni-filtered Cu Kα radiation.

Mesophase observations were obtained with an optical microscope (Olympus BH-2) fitted with crossed polarizers. The temperature was controlled to ±1°C by means of a computerized Linkam THM 600 heat controller.

The synchrotron radiation measurements ($\lambda = 150$ Å) were performed at HASYLAB DESY (Hamburg, Germany) with a position-sensitive one-dimensional detector at a

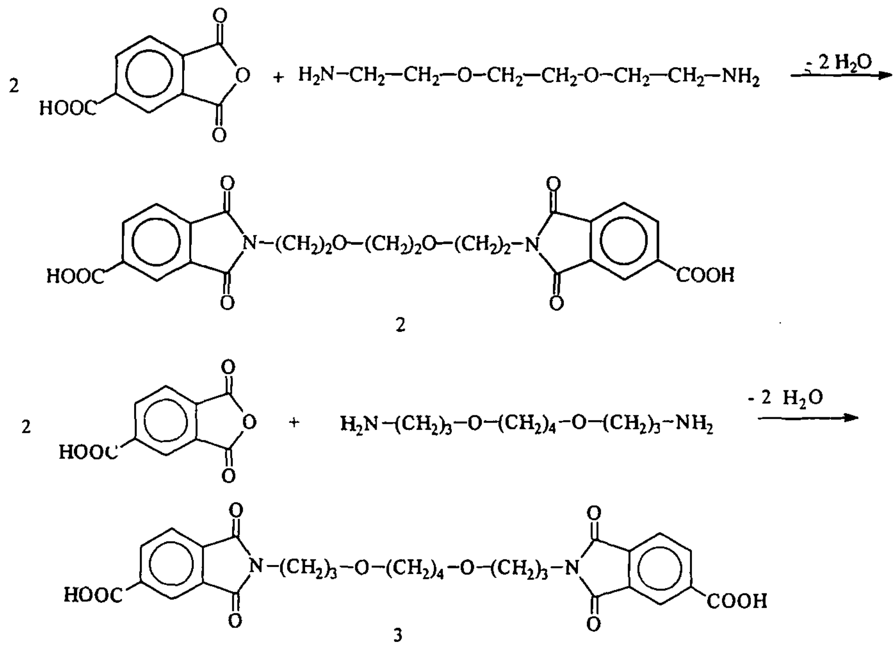

Scheme 1

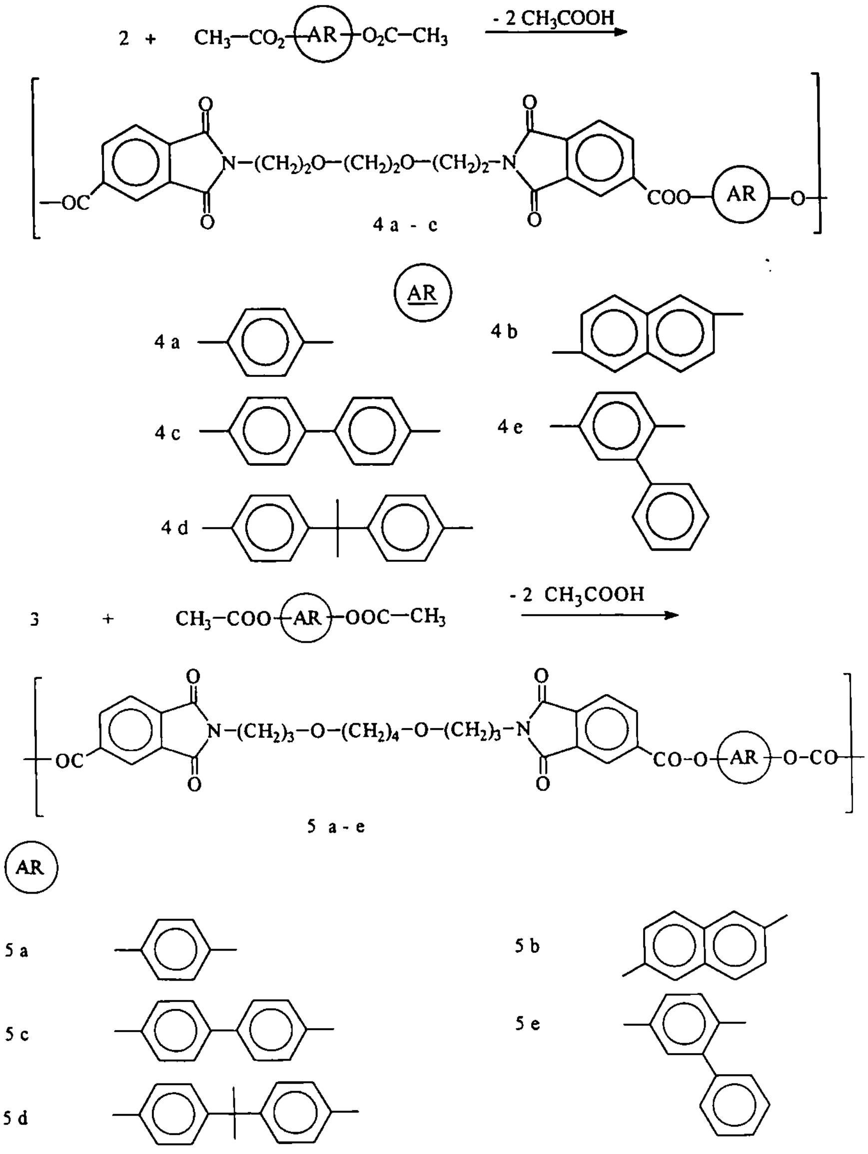

Scheme 2

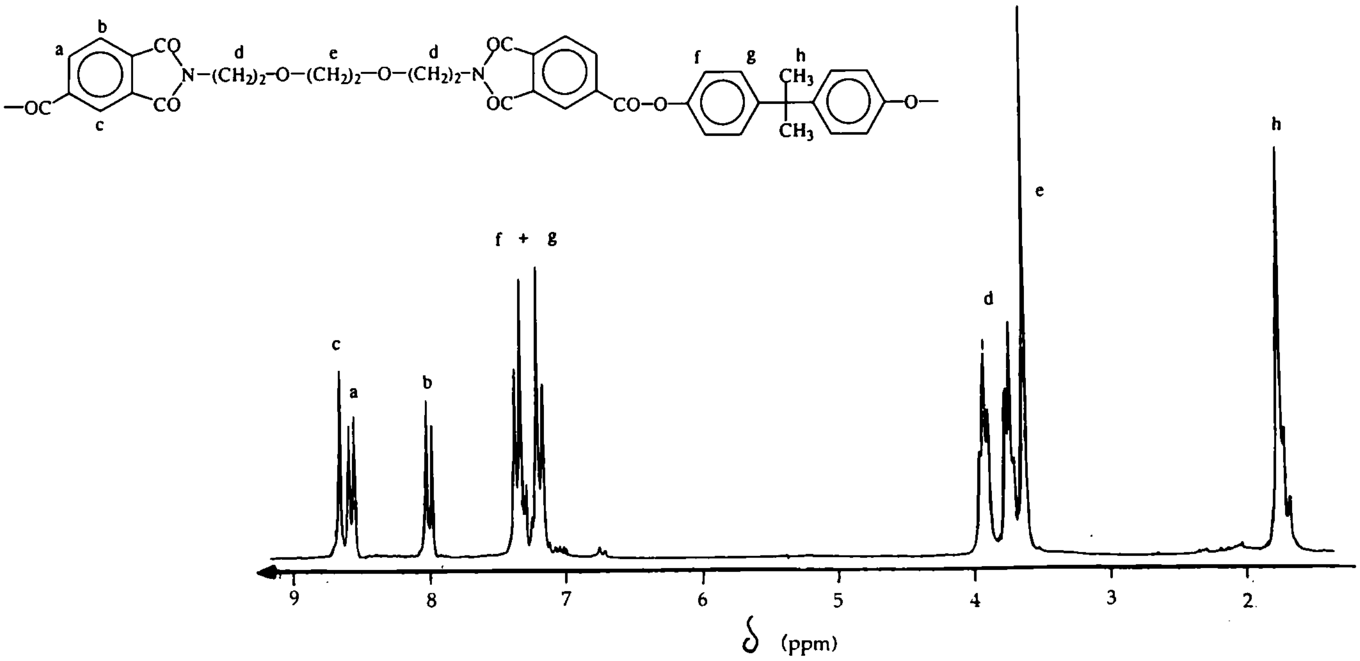

Figure 1 200 MHz ^1H n.m.r. spectrum of poly(ester imide) **4d** (measured in $CDCl_3$/trifluoroacetic acid)

Table 1 Poly(ester imide)s from **2** and bisphenol diacetates

Polymer	Yield (%)	η_{inh} (dl g^{-1})	T_g (°C)	T_m (°C)	T_i (°C)	Elemental formula (mol. weight)	Elemental analyses	C	H	N
4a	86	0.54	105	290	–	$C_{30}H_{22}N_2O_{10}$	Calc.	63.16	3.86	4.91
				294^a		(570.51)	Found	62.95	4.10	4.87
4b	98	0.47	105	320	–	$C_{34}H_{24}N_2O_{10}$	Calc.	65.81	3.87	4.51
				295		(620.57)	Found	64.98	4.03	4.40
4c	88	0.35	109	310	385	$C_{36}H_{26}N_2O_{10}$	Calc.	66.87	4.03	4.33
				309^a	384^a	(646.61)	Found	66.58	4.30	4.27
4d	88	0.41	118	–	–	$C_{36}H_{26}N_2O_{10}$	Calc.	66.87	4.03	4.33
						(646.61)	Found	66.58	4.12	4.27
4e	84	0.37	105	–	–	$C_{39}H_{32}N_2O_{10}$	Calc.	68.02	4.65	4.07
						(688.69)	Found	68.09	5.13	3.94

^{a} As observed under the polarizing microscope

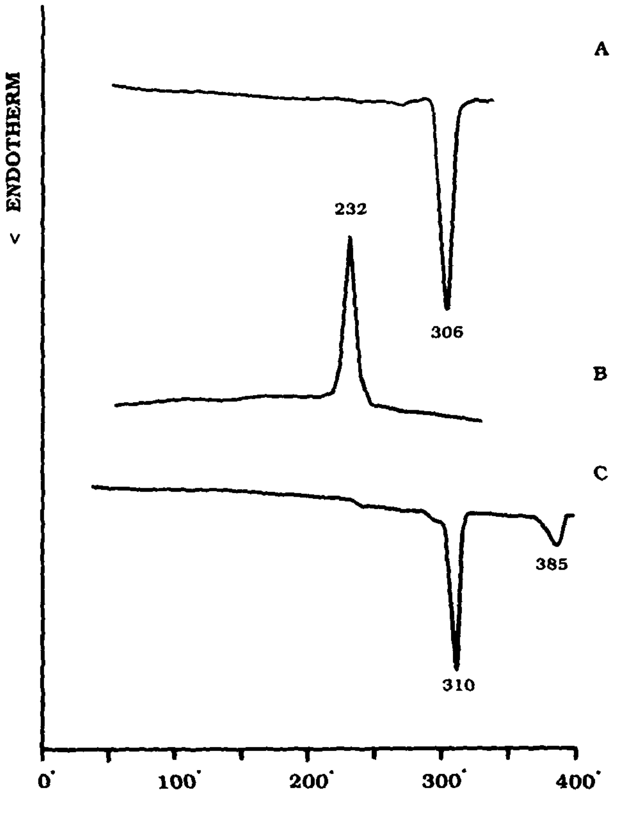

Figure 2 D.s.c. measurements (heating and cooling rate 20°C min^{-1}) of poly(ester imide) **4c**: (A) first heating; (B) first cooling; (C) first heating of a fresh sample

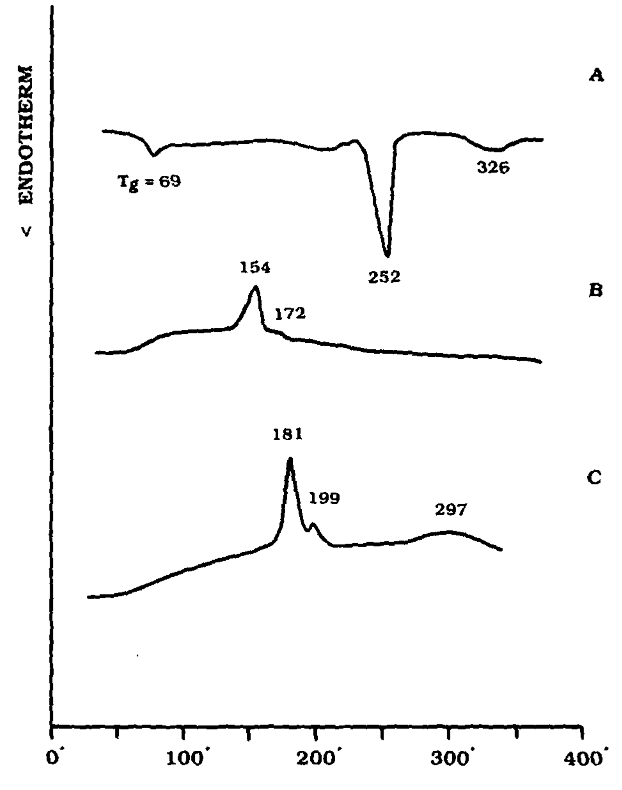

Figure 3 D.s.c. measurements (heating and cooling rate 20°C min^{-1}) of poly(ester imide) **5c**: (A) first heating to 370°C; (B) first cooling from 370°C; (C) first cooling of a second sample after heating to 330°C

heating or cooling rate of 20°C min^{-1}. Computer modelling of repeating units was conducted with the force-field program 'Insight II-Discover' (Biosym).

RESULTS AND DISCUSSION

Synthesis of monomers and polymers

Monomers **2** and **3** were synthesized from the corresponding commercial diamines and trimellitic anhydride by a one-pot procedure using acetic acid as solvent and without the addition of dehydrating agents or any other promoter for imide ring closure (*Scheme 1*). They have not been described previously in the literature and showed moderate melting points, allowing polycondensations in the melt without thermal decomposition.

Two series of PEIs, **4a–e** and **5a–e**, were prepared from the diacid imides **2** and **3** and a set of acetylated commercial bisphenols (*Scheme 2*). Freshly recrystallized starting materials were used, and a catalytic amount of MgO was added to the polymerization mixture in every case.

Since the aliphatic ether units show limited thermal resistance, temperatures over 280°C were never applied, so that the last steps of the reaction proceeded in the solid state in most cases, and agitation could not be maintained over the whole course of the

Table 2 Poly(ester imide)s from **3** and bisphenol diacetates

Polymer	Yield (%)	η_{inh} (dl g^{-1})	T_g (°C)	T_m (°C)	T_i (°C)	Elemental formula (mol. weight)	Elemental analyses	C	H	N
5a	87	0.32	56	184	–	$C_{34}H_{30}N_2O_{10}$ (626.62)	Calc. Found	65.18 65.02	4.79 5.01	4.47 4.46
5b	90	0.23	68	200	–	$C_{38}H_{32}N_2O_{10}$ (676.68)	Calc. Found	67.46 66.79	4.73 5.05	4.14 3.80
5c	91	0.30	70	252 220^a	326 315–25^a	$C_{40}H_{34}N_2O_{10}$ (702.72)	Calc. Found	68.38 68.09	4.84 5.00	3.99 4.10
5d	98	0.33	60	–	–	$C_{40}H_{34}N_2O_{10}$ (702.72)	Calc. Found	68.37 68.08	4.84 5.21	3.99 4.14
5e	87	0.30	71	–	–	$C_{43}H_{40}N_2O_{10}$ (744.80)	Calc. Found	69.35 69.11	5.38 5.66	3.76 3.48

^{a} As observed under the polarizing microscope

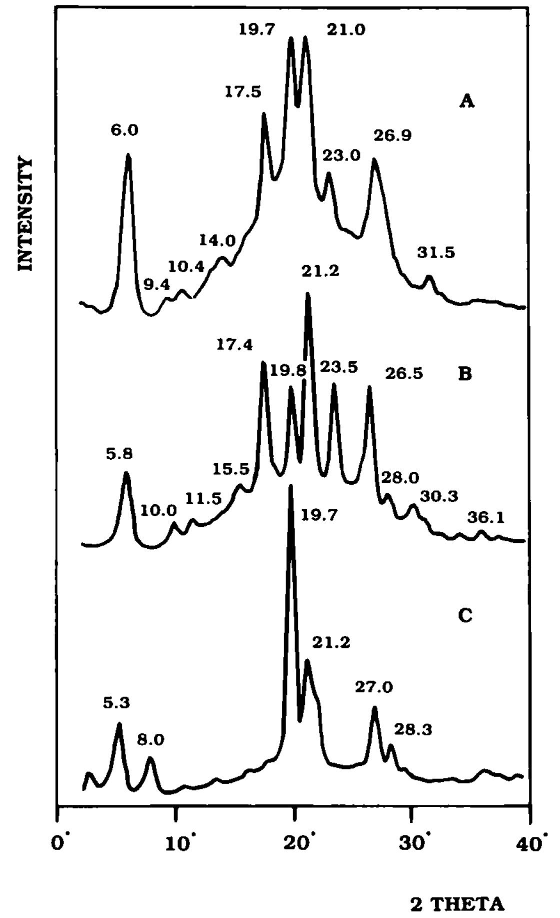

Figure 4 WAXD powder patterns of poly(ester imide)s: (A) **4a**; (B) **4b**; (C) **4c**

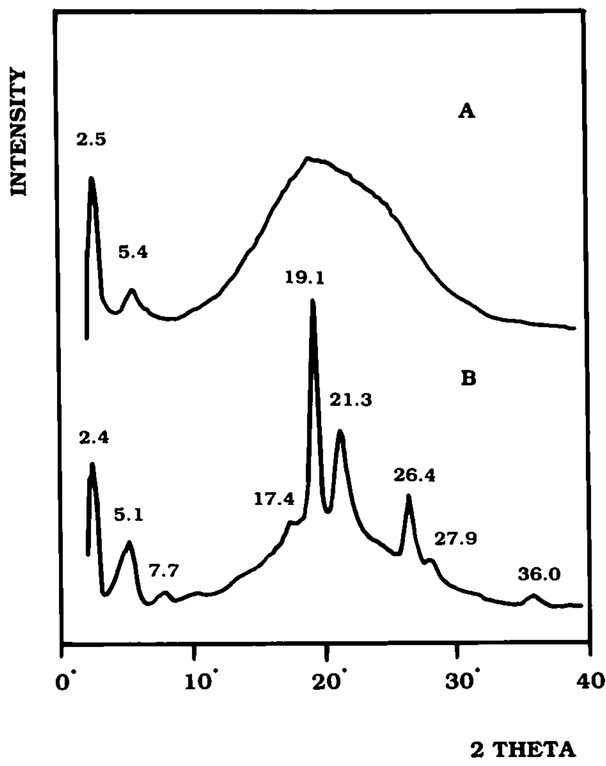

Figure 5 WAXD powder pattern of poly(ester imide) **5b**: (A) after cooling from the isotropic melt at 20°C min^{-1}; (B) after annealing at 130°C for 20 h

polycondensation. The method did indeed prevent thermal decomposition, but on the other hand, high molecular weights were not achieved. Inherent viscosities in the range 0.3–0.5 dl g^{-1} must be considered as moderate to low viscosities. In spite of that, signals attributable to end groups were hardly detected in ^1H n.m.r. spectra. As an example, the spectrum of polymer **4d** is shown in *Figure 1*. Yields and properties of PEIs **4a–e** are summarized in *Table 1* and those of PEIs **5a–e** in *Table 2*.

Characterization

Polymers **4a–e** and **5a–e** were soluble in strong protonated acids and mixtures of TFA/chlorinated hydrocarbons, and in aprotic polar solvents such as dimethylsulfoxide or *N*-methylpyrrolidone. Thus, they are more soluble than PEIs of series **1** that are insoluble in aprotic organic solvents.

The effect of the –O– linkages within the repeat unit of the current PEIs could be also observed when their thermal behaviour was investigated by d.s.c. In all cases an inflection of the d.s.c. curve was observed, in the range 100–120°C for polymers **4a–e**, and 50–70°C for polymers **5a–e**, that was assigned to the glass transition temperature (T_g). These values are lower than those measured for the analogous PEIs derived from monomer **1**. This result is

Table 3 Middle angle reflections (2ϑ) and layer distances (*d*-spacings, Å) calculated according to the Bragg equation

Diphenol		5a–c 2ϑ	5a–c *d* (Å)	4a–c 2ϑ	4a–c *d* (Å)
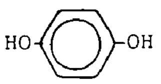	1.Ord.	2.6	33.8	–	–
	2.Ord.	5.3	33.3	6.0	29.5
	3.Ord.	–	–	–	–
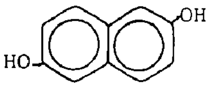	1.Ord.	2.4(5)	36.0	–	–
	2.Ord.	5.1	34.6	5.8	30.5
	3.Ord.	7.7	34.4	–	–
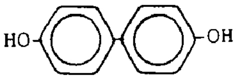	1.Ord.	2.3(5)	37.8	–	–
	2.Ord.	4.7	37.6[a]	5.3	33.2[b]
	3.Ord.	7.1	37.4	8.0	33.1

[a] Calculated for a fully extended repeating unit ($\alpha = 180$ in *Figures 11* and *12*): $d = 36.5$ Å for the all-*gauche* and 40.2 Å for the all-*trans* conformation

[b] Calculated for a fully extended repeating unit ($\alpha = 180$ in *Figures 11* and *12*): $d = 33.3$ Å for the all-*gauche* and 35.0 Å for the all-*trans* conformation

Figure 6 Smectic texture of poly(ester imide) **5c** in the melt at 280 C

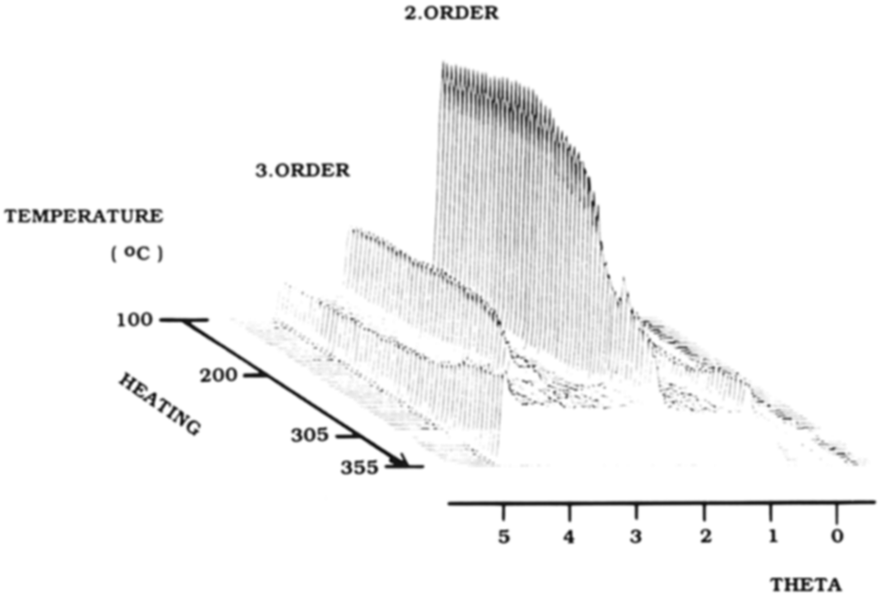

Figure 7 WAXD measurements of poly(ester imide) **4c** with synchrotron radiation at a heating rate of $20\ \mathrm{C\ min^{-1}}$

reasonable, because ether linkages are known to improve the flexibility of aliphatic or aromatic chains.

With regard to crystallinity the PEIs of this work may be subdivided into two classes. The PEIs **4d**, e and **5d**, **e** are amorphous and even annealing for 2 h above T_g did not induce crystallization. This result was not unexpected for the PEIs of bisphenol-A, but it was unpredictable for the PEIs derived from phenylhydroquinone. The PEIs of the other three diphenols proved to be semicrystalline showing a melting endotherm in the d.s.c. heating trace and a crystallization exotherm in the cooling trace (*Figures 2* and *3*). A characteristic difference between series **4a–c** and **5a–c** concerns the melting temperature (T_m). Whereas the T_ms of **4a–c** fall into a narrow temperature range those of **5a–c** display a significant increase in this order (*Table 2*). However, **4a–c** and **5a–c** have in common that the wide-angle X-ray diffraction (WAXD) powder patterns exhibit a middle angle reflection which indicates the existence of a layer structure in the solid state (*Figures 4* and *5*). Similar layer structures have already been reported for the PEIs derived from monomer **1**. The layer distances (*d*-spacings) calculated via the Bragg equation are compiled in *Table 3*. As discussed below, the X-ray data suggest that the mesogens are not significantly tilted relative to the layer plane.

A characteristic difference between **4c** or **5c**, on the one hand, and **4a, b** or **5a, b**, on the other hand, is the extremely rapid crystallization of **4c** and **5c**. Even quenching from the melt does not prevent crystallization. The same observation has been made for PEIs derived from **1** ($n = 10$ or 12) and 4,4′-dihydroxybiphenyl. In the case of **4a, b** or **5a, b** quenching from the melt suppresses the crystallization, and in the case of **5b** even cooling with a rate of $-20°C\,min^{-1}$ prevents crystallization almost completely (*Figure 5*).

The rapid crystallization of **4c** and **5c** is obviously a consequence of the thermotropic character of both PEIs. As evidenced by optical microscopy with crossed polarizers, **4c** and **5c** form a mobile smectic melt (*Figure 6*). The texture of this smectic phase is identical for both **4c** and **5c** and suggests the formation of a smectic-A phase. In this connection it should be emphasized that in the case of LC main chain polymers, contrary to LC side chain polymers, only smectic-A and smectic-C phases yield a mobile melt. All other smectic phases form solid mesophases. The observed texture and its relatively high mobility as observed by shearing between glass plates suggests a smectic-A rather than a smectic-C phase.

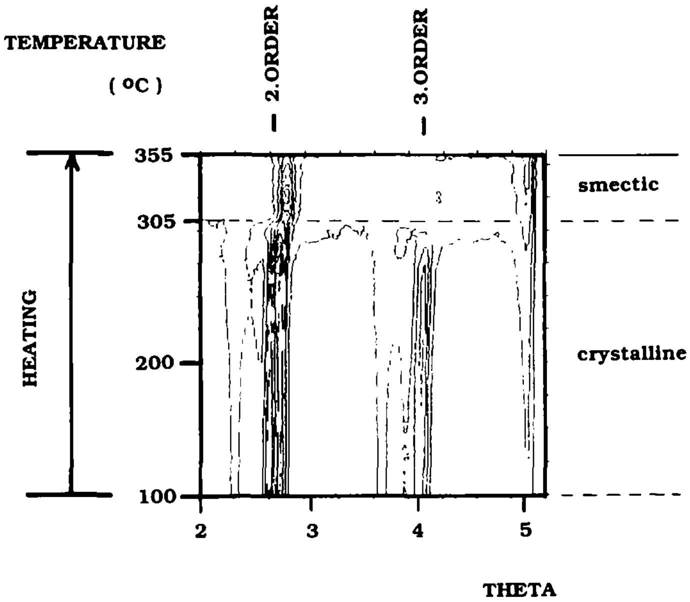

Figure 8 Contour map of the WAXD measurements of 4c presented in *Figure 7*

Optical microscopy, X-ray and d.s.c. measurements agree in that heating of **4c** up to the isotropic state results in rapid thermal degradation. Neither anisotropization nor a crystallization exotherm is detectable in the cooling trace when **4c** was heated above 400°C. However, an almost complete crystallization exotherm is observable when the heating was stopped immediately above T_m (*Figure 2*). The longer spacer of **5c** lowers the phase transition temperatures. Yet, even here, heating to 370°C (*Figure 3A*) prevents the appearance of an anisotropization exotherm in the cooling trace, and the melting exotherm is considerably reduced (*Figure 3B*). When the heating was stopped at 330°C, the anisotropization is detectable in the cooling trace and the crystallization exotherm has doubled in size (*Figure 3C*). Although the thermostability of both PEIs is low above 300°C, this did not hinder the characterization of the LC phase.

When synchrotron radiation measurements of **4c** and **5c** were conducted with a heating rate of $20°C\,min^{-1}$ (*Figures 7–10*), the lower transition temperatures of **5c** also allowed the measurement of the cooling process (*Figure 10*). These synchrotron radiation measurements display middle angle reflections for the melt of both **4c** and **5c**, and thus confirm the existence of an enantiotropic, smectic LC phase. In both cases, the middle angle reflections shift to somewhat higher values upon melting indicating a shortening of the layer distances. This effect is weak (~1 Å) in the case of **4c** and amounts to ~1.5 Å in the case of **5c** (*Figure 10*). A proper interpretation of

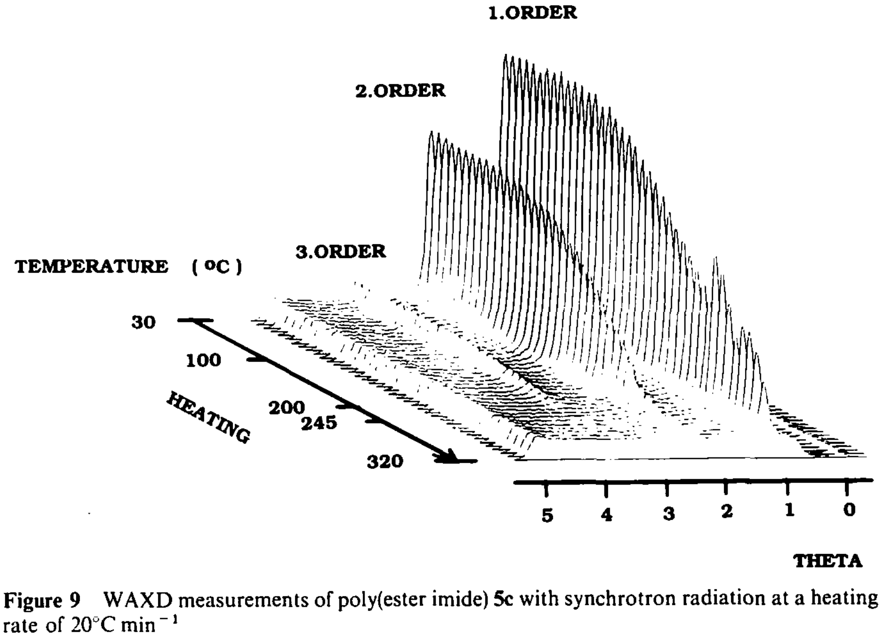

Figure 9 WAXD measurements of poly(ester imide) 5c with synchrotron radiation at a heating rate of $20°C\,min^{-1}$

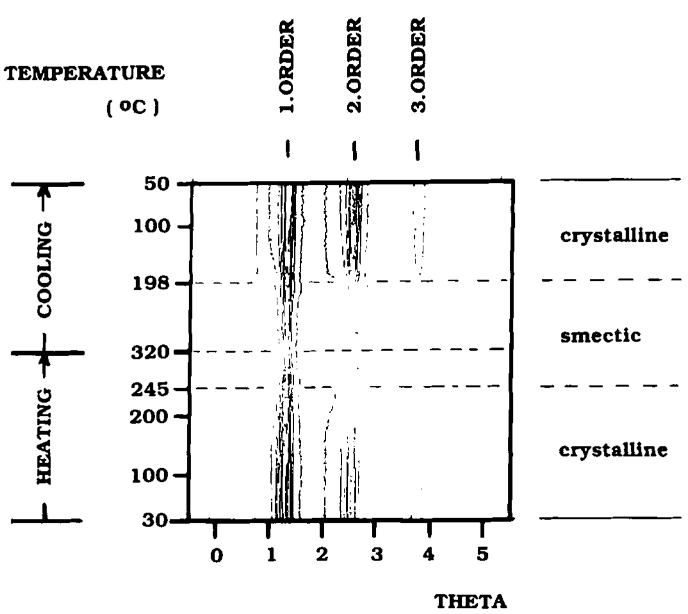

Figure 10 Contour map of the WAXD measurements of **5c** presented in *Figure 9*

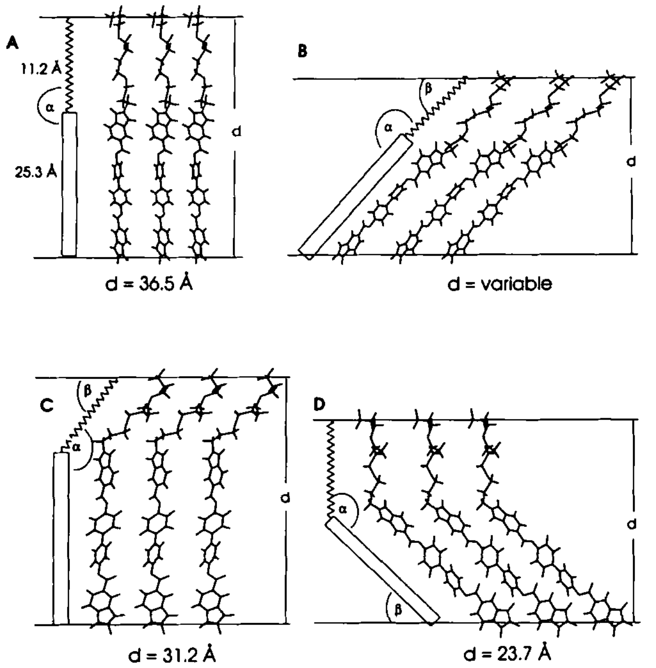

Figure 11 Four different kinds of chain packing calculated for **5c** with a force-field program assuming an all-*gauche* conformation for the spacer (α = 180° in A and B, α = 142° in C and D)

this change requires the knowledge of the chain packing in the solid state.

The WAXD powder patterns of **4c** and **5c** (*Figures 4*, *7* and *9*) exclude a hexagonal type of chain packing. As a consequence, the solid state is either a smectic-E phase (upright mesogens) or a smectic-H phase (tilted mesogens). In contrast to low molecular weight LC compounds the repeating units of PEIs are not necessarily linear under all circumstances (α = 180° in *Figures 11* and *12*). Computer modelling with a force-field program yielded an angle α of 122° for spacers in all-*gauche* conformation (*Figures 11C* and *D*) or α = 142° for spacers in all-*trans* conformation (*Figures 12C* and *D*) as the energy minimum. Even if the absolute values are not taken too seriously they clearly indicate a tendency of the repeating units to deviate from linearity. The formation of a linear repeating unit requires little energy, and thus the crystallization might enforce an almost linear repeating unit (*Figures 11A* and *B* or *12A* and *B*). If so, the slight shortening of the *d*-spacings at the melting point of **4c** and **5c** might result from the change of an almost linear to a more angular repeating unit (A→C transition in *Figures 11* and *12*).

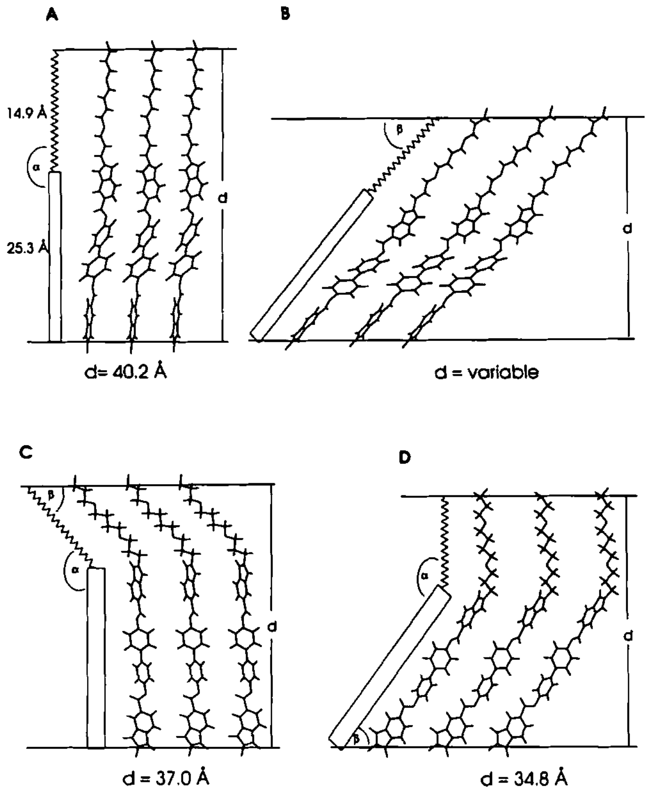

Figure 12 Four different kinds of chain packing calculated for **5c** with a force-field program assuming an all-*trans* conformation for the spacer (α = 180° in A and B, α = 122° in C and D)

The question if the mesogens are tilted cannot be answered on the basis of WAXD patterns alone, because the conformation of the spacers is another important factor influencing the *d*-spacings and the WAXD patterns do not give any information on the conformations of the spacers. However, it is well known that poly(ethylene oxide)s prefer *gauche* to *trans* conformations because of the unfavourable interaction between the α-electrons of the oxygen and the C–H σ-bonds in the β-position. Therefore, four different models of chain packing were calculated with all-*gauche* conformation of the spacers (*Figure 11*) and another set with all-*trans* conformation (*Figure 12*). The experimental data (*Table 3*) fit surprisingly well with *d*-spacings calculated for model A of *Figure 11*. However, X-ray data alone do not exclude model C of *Figure 12*. However, an all-*trans* conformation of the spacers is extremely unlikely. In other words the X-ray data suggest, in agreement with optical microscopy, that **4c** and **5c** form a smectic-E phase in the solid state and a smectic-A phase with α < 180° in the melt. However, the above interpretation should not be considered as conclusively proven.

CONCLUSIONS

The results discussed above clearly demonstrate that only the PEIs **4c** and **5c** form an enantiotropic LC phase, which is most likely a smectic-A phase. When compared to PEIs derived from monomer **1** two interesting differences are noteworthy. First, the temperature range of the LC phase of **4c** and **5c** is smaller. Secondly, in the case of monomer **1** even the PEIs derived from hydroquinone or 2,6-dihydroxynaphthalene are thermotropic. In other words, ether groups in the spacer considerably reduce the tendency of PEIs to form layer structures.

From this point of view, the results of this work agree well with those found for PEIs **6** and **7**[8,11]. Obviously a good compatibility between the polar imide mesogens and the ether spacers is responsible for this tendency. This effect was not predictable, because other polyesters based on oligo(ethylene oxide) spacers (e.g. **8**[3] and **9**[5–7]) form layer structures in the solid and liquid state.

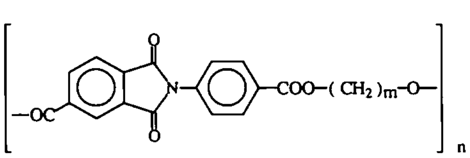

6

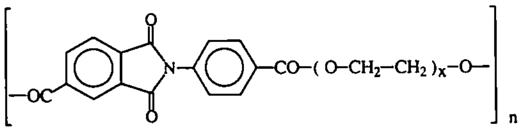

7

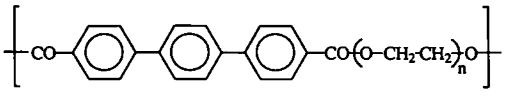

8

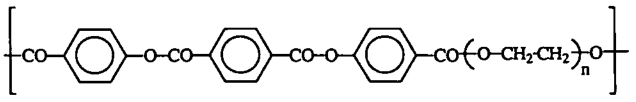

9

ACKNOWLEDGEMENTS

We wish to thank Dipl.-Chem. V. Linzer for computer modelling and the Alexander von Humboldt-Stiftung for financial support.

REFERENCES

1 Kricheldorf, H. R. and Pakull, R. *Polymer* 1987, **28**, 1772

2 Kricheldorf, H. R. and Pakull, R. *Macromolecules* 1988, **21**, 551

3 Noël, C., Friedrich, C., Bosio, L. and Strazielle, L. *Polymer* 1984, **25**, 1281

4 Kalika, D. S., Shen, M.-R., Denn, M. M., Janelli, P., Masciocchi, N., Yoon, D. Y., Porrish, W., Friedric, C. and Noël, C. *Macromolecules* 1990, **23**, 5192

5 Delvin, A., Ober, C. K. and Bluhm, T. L. *Macromolecules* 1989, **22**, 498

6 Jedlinski, Z., Franck, J., Kulczycki, A., Sirigu, A. and Carfagna, C. *Macromolecules* 1989, **22**, 1600

7 Minkova, L., Mihailov, M. and Jedlinski, Z. *Acta Polym.* 1992, **43**, 8

8 Kricheldorf, H. R., Schwarz, G., Berghahn, M., de Abajo, J. and de la Campa, J. *Macromolecules* 1994, **27**, 2540

9 Richard, W. W. *Org. Synth. Coll.* 1955, **3**, 452

10 Riande, E., Guzmán, J. and de Abajo, J. *Makromol. Chem.* 1984, **185**, 1943

11 Kricheldorf, H. R., Schwarz, G., de Abajo, J. and de la Campa, J. *Polymer* 1991, **32**, 942